

Supporting information

CuSCN as Selective Contact in Solution Processed Small Molecule Organic Solar Cells Leads to over 7% Efficient Porphyrin Based Device.

Gabriela Morán^a, Susana Arrechea^a, Pilar de la Cruz^a, Virginia Cuesta,^a S. Biswas^d, Emilio Palomares^{b,c*}, Ganesh D. Sharma^{d*}, Fernando Langa^{a*}

^aUniversidad de Castilla-La Mancha. Institute of Nanoscience, Nanotechnology and Molecular Materials (INAMOL), Campus de la Fábrica de Armas, Toledo. Spain. Tel: 34 9252 68843. E-mail: Fernando.Langa@uclm.es

^bInstitute of Chemical Research of Catalonia (ICIQ). Avda. Països Catalans, 14. Tarragona. E-43007. Spain. E-mail: epalomares@ICIQ.ES epalomares@ICIQ.ES

^cICREA. Passeig Lluis Companys, 23. Barcelona. E-08010. Spain.

^dDepartment of Physics, The LNM Institute of Information Technology (Deemed University), Rupa ki Nagal, Jamdoli, Jaipur (Raj.) 302031, India

Table of contents

1. Experimental details	S1-S2
2. ^1H -NMR, ^{13}C-NMR, FT-IR and MALDI-TOF or MS spectra	S3
3. Thermogravimetric analysis	S14
4. UV-Visible and emission spectroscopies	S14
5. Square Wave plots	S16

Experimental details

Synthetic procedures were performed under Argon atmosphere, in dry solvent unless otherwise noted. All reagents and solvents were reagent grade and were used without further purification. Chromatographic purifications were performed using silica gel 60 SDS (particle size 0.040-0.063 mm). Analytical thin-layer chromatography was performed using Merck TLC silica gel 60 F254. ^1H -NMR spectra were obtained on Bruker TopSpin AV-400 (400 MHz) spectrometer. Chemical shifts are reported in parts per million (ppm) relative to the solvent residual peak (CDCl_3 , 7.27 ppm). ^{13}C -NMR chemical shifts (δ) are reported relative to the solvent residual peak (CDCl_3 , 77.0 ppm). UV-Vis measurements were carried out on a Shimadzu UV 3600 spectrophotometer. For extinction coefficient determination, solutions of different concentration were prepared in CH_2Cl_2 .

(HPLC grade) with absorption between 0.1-1 of absorbance using a 1 cm UV cuvette. The emission measurements were carried out on Cary Eclipse fluorescence spectrophotometer. Mass spectra (MALDI-TOF) were recorded on a VOYAGER DETM STR mass spectrometer using dithranol as matrix. Melting points are uncorrected.

Cyclic voltammetry was performed in ODCB-acetonitrile (4:1) solutions. Tetrabutylammonium perchlorate (0.1 M as supporting electrolyte) were purchased from Acros and used without purification. Solutions were deoxygenated by argon bubbling prior to each experiment, which was run under argon atmosphere. Experiments were done in a one-compartment cell equipped with a platinum working microelectrode ($\varnothing = 2$ mm) and a platinum wire counter electrode. An Ag/AgNO₃ (0.01 M in CH₃CN) electrode was used as reference and checked against the ferrocene/ferrocenium couple (Fc/Fc⁺) before and after each experiment.

The thermal stability was evaluated by TGA on a Mettler Toledo TGA/DSC Start^e System under nitrogen, with a heating rate of 10 °C/min. Heating of crystalline sam

3. ^1H NMR, ^{13}C NMR, FT-IR and MALDI-TOF MS spectra

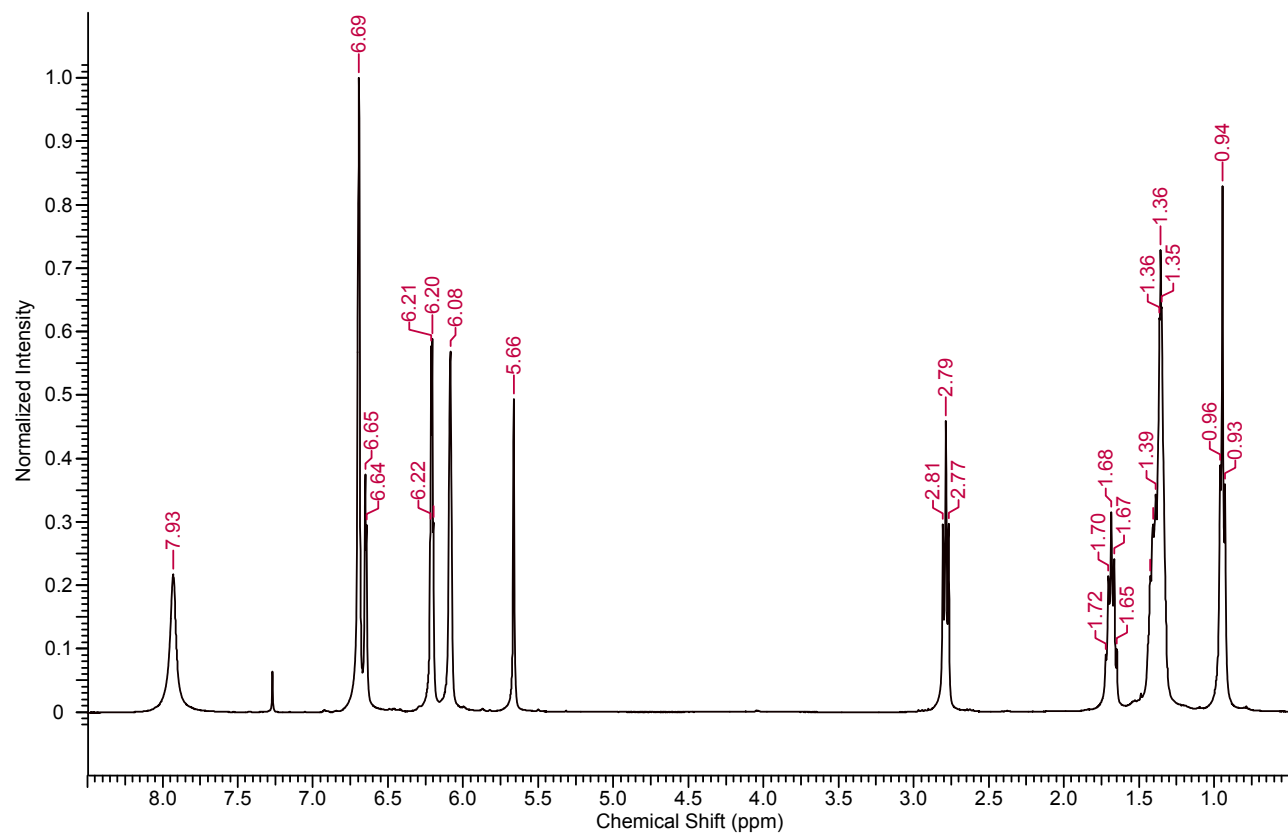


Figure S1. ^1H NMR spectrum (400 MHz, CDCl_3) of **3**.

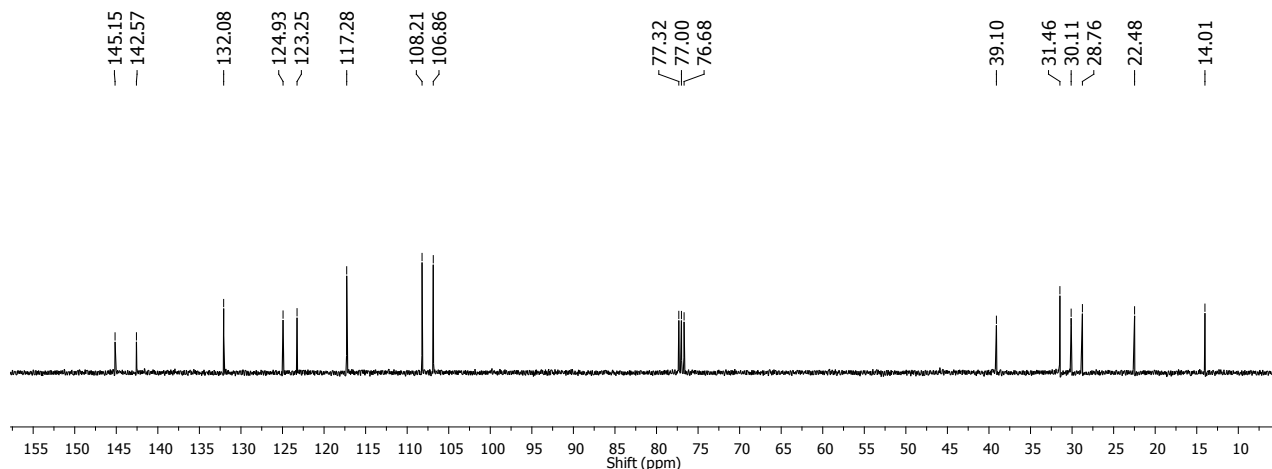


Figure S2. ^{13}C NMR spectrum (100 MHz, CDCl_3) of **3**.

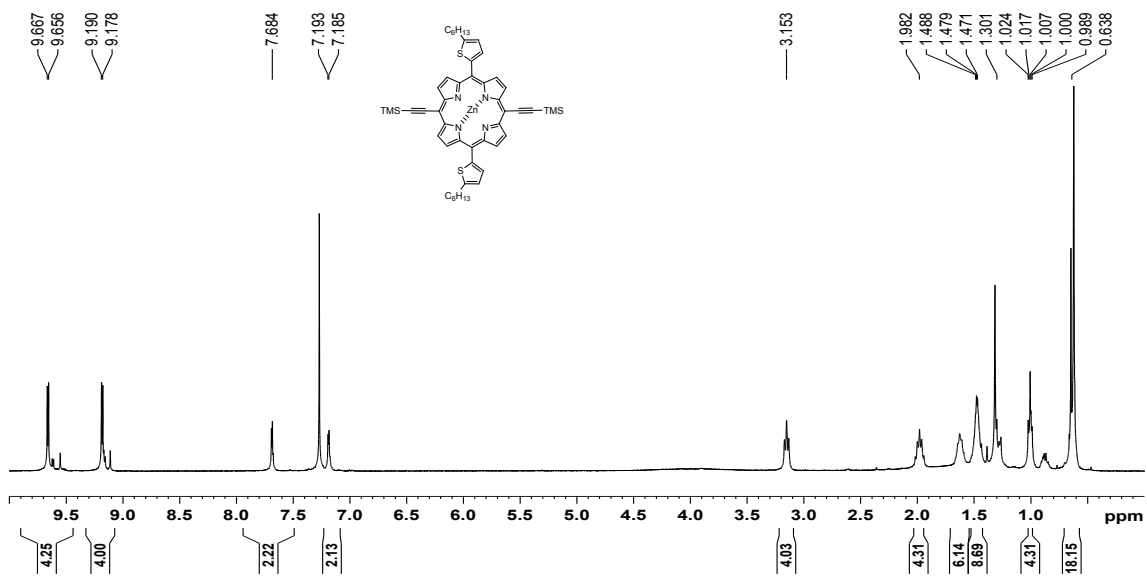


Figure S3. ^1H NMR spectrum (400 MHz, CDCl_3) of **6**.

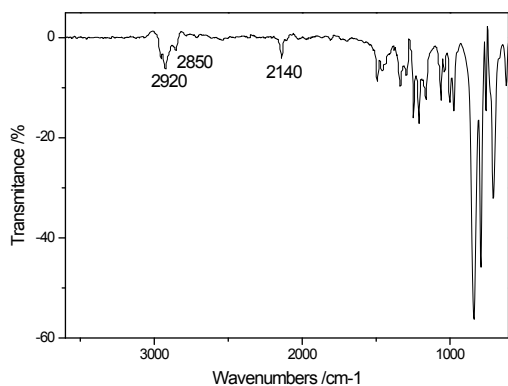


Figure S4. FT-IR spectrum of compound **6**.

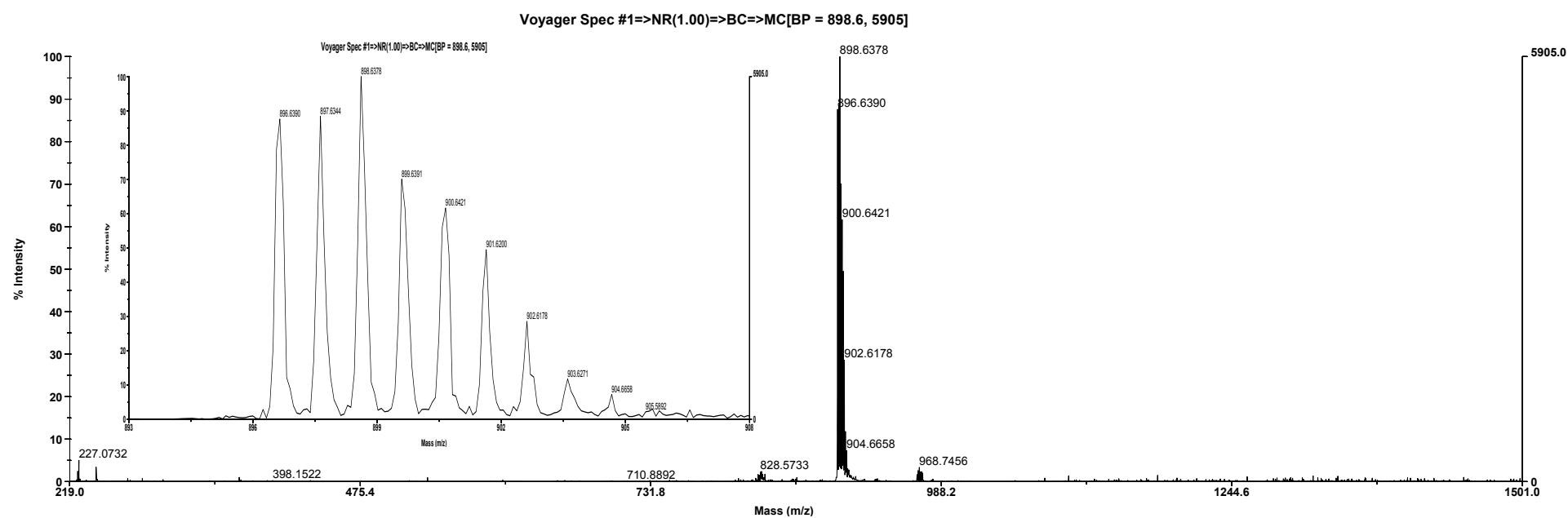


Figure S5. MALDI-TOF MS spectrum of compound **6** (Matrix: Dithranol).

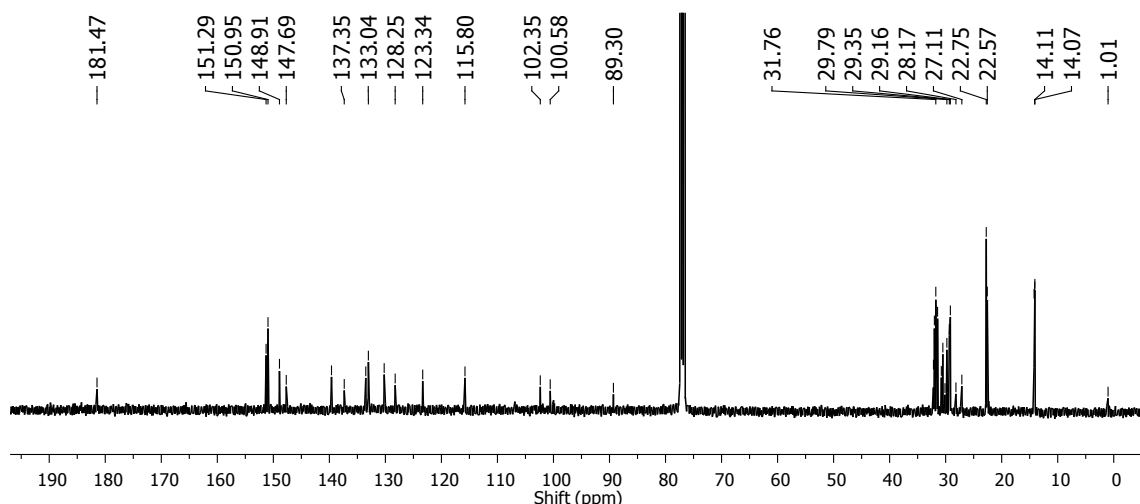
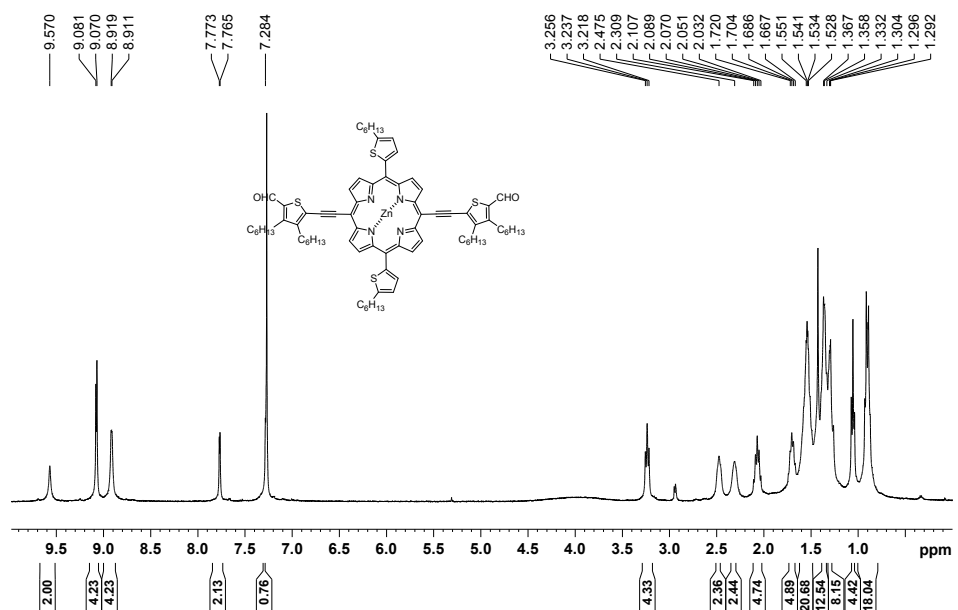


Figure S7. ^{13}C NMR spectrum (100 MHz, CDCl_3) of **8a**.

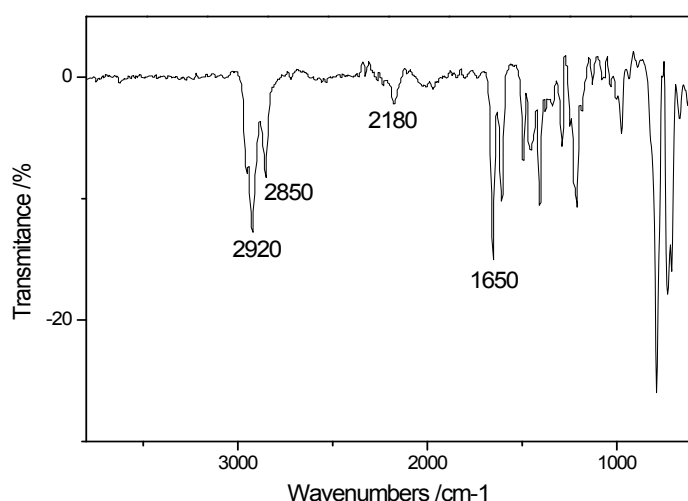


Figure S8. FT-IR spectrum of compound **8a**.

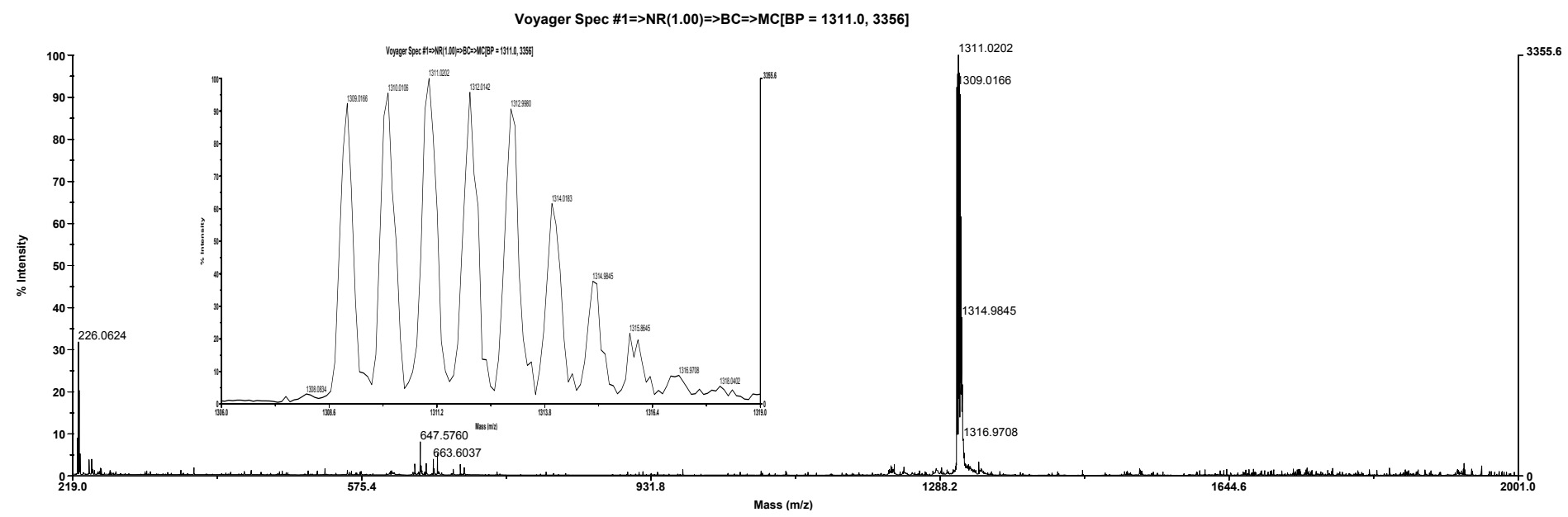


Figure S9. MALDI-TOF MS spectrum of compound **8a** (Matrix: Dithranol).

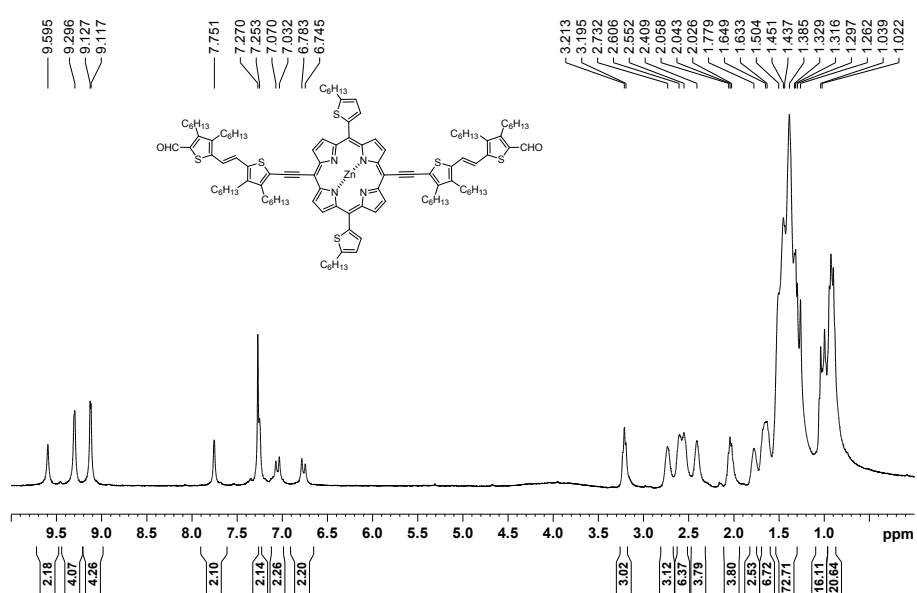


Figure S10. ^1H NMR spectrum (400 MHz, CDCl_3) of **8b**.

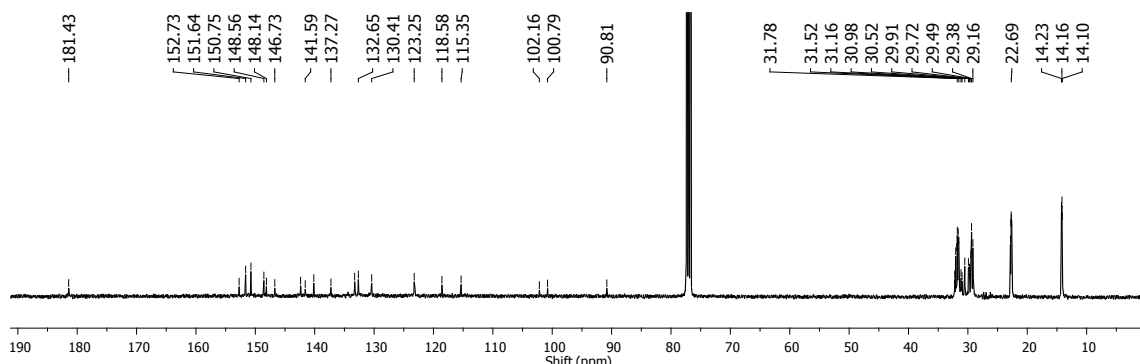


Figure S11. ^{13}C NMR spectrum (100 MHz, CDCl_3) of **8b**.

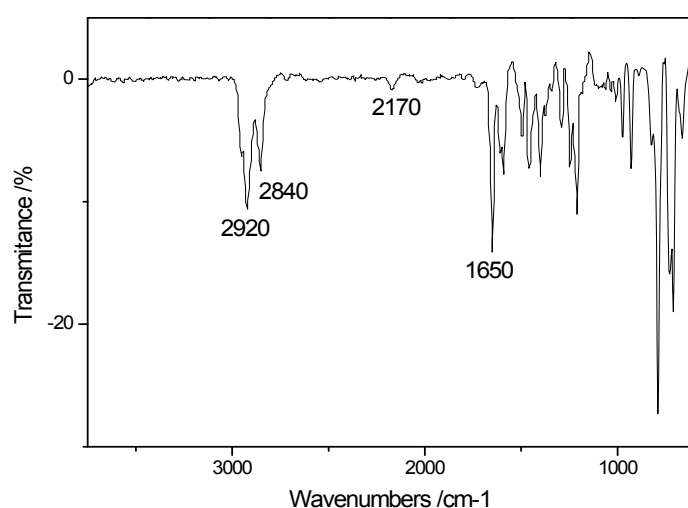


Figure S12. FT-IR spectrum of compound **8b**.

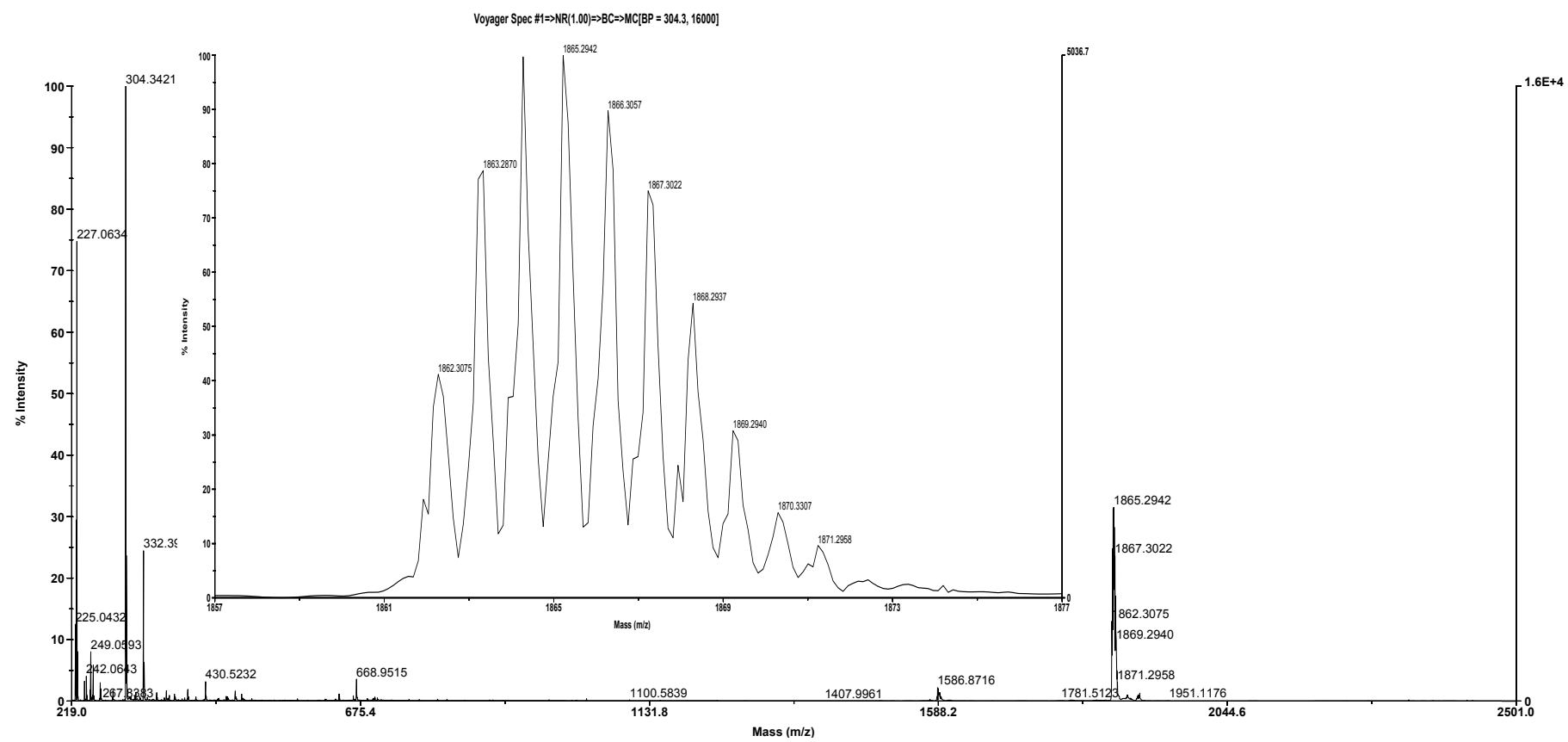


Figure S13. MALDI-TOF MS spectrum of compound **8b** (Matrix: Dithranol).

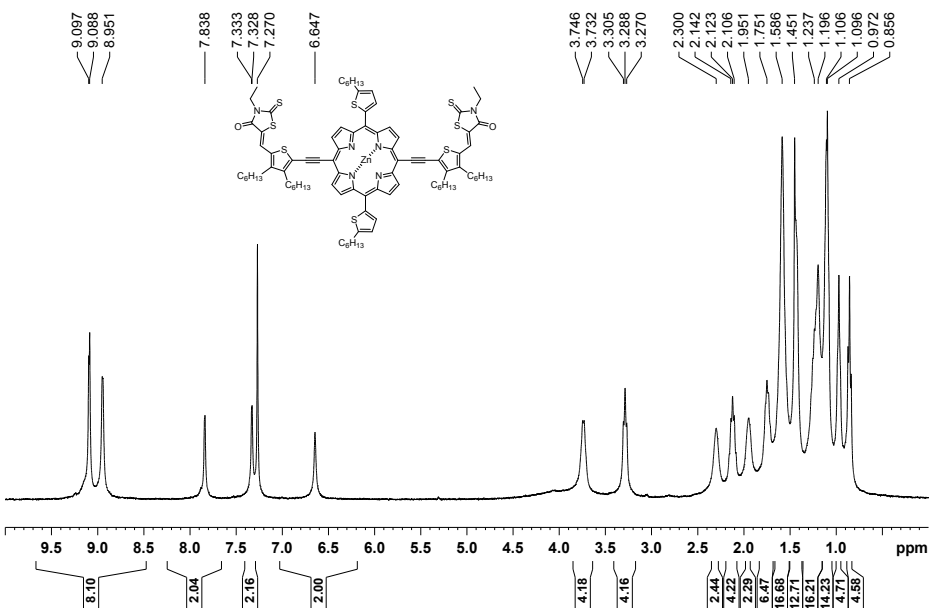


Figure S14. ¹H NMR spectrum (400 MHz, CDCl₃) of **1a**

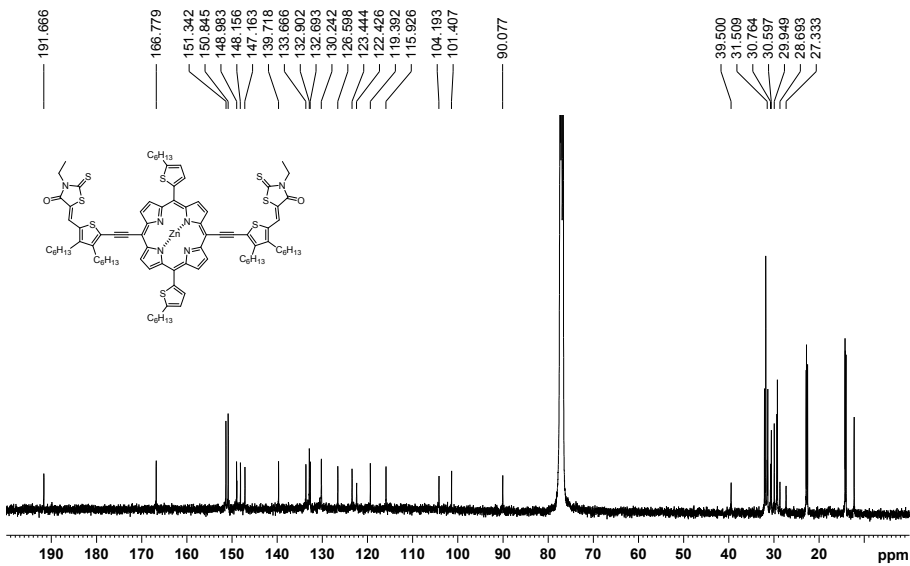


Figure S15. ¹³C NMR spectrum (100 MHz, CDCl₃) of **1a**

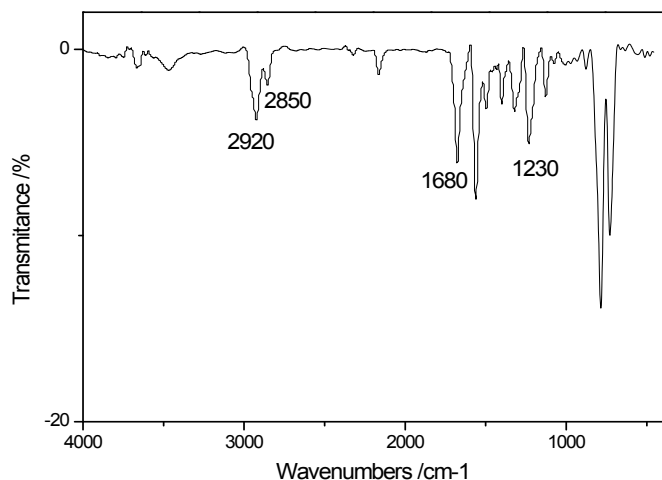


Figure S16. FT-IR spectrum of compound **1a**.

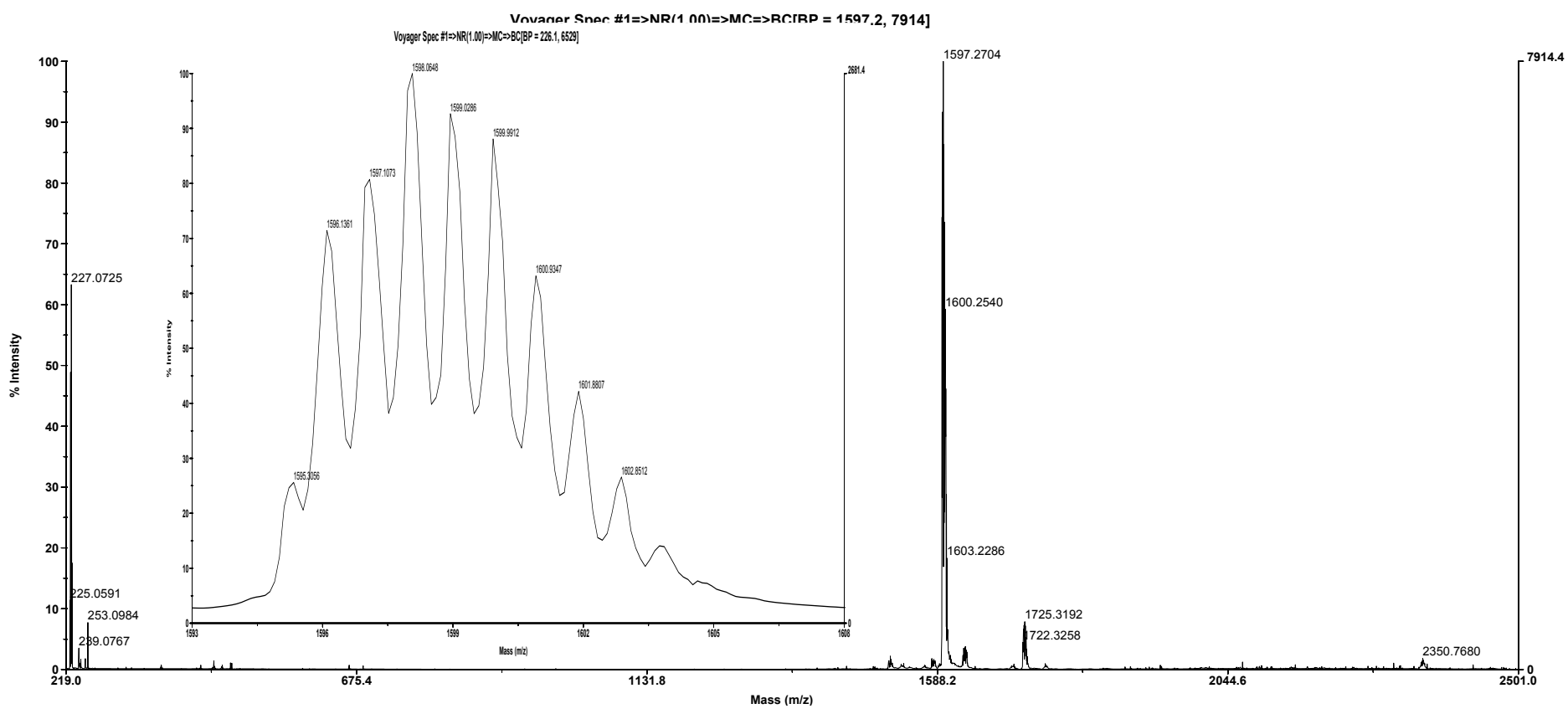


Figure S17. MALDI-TOF MS spectrum of compound **1a** (Matrix: Dithranol).

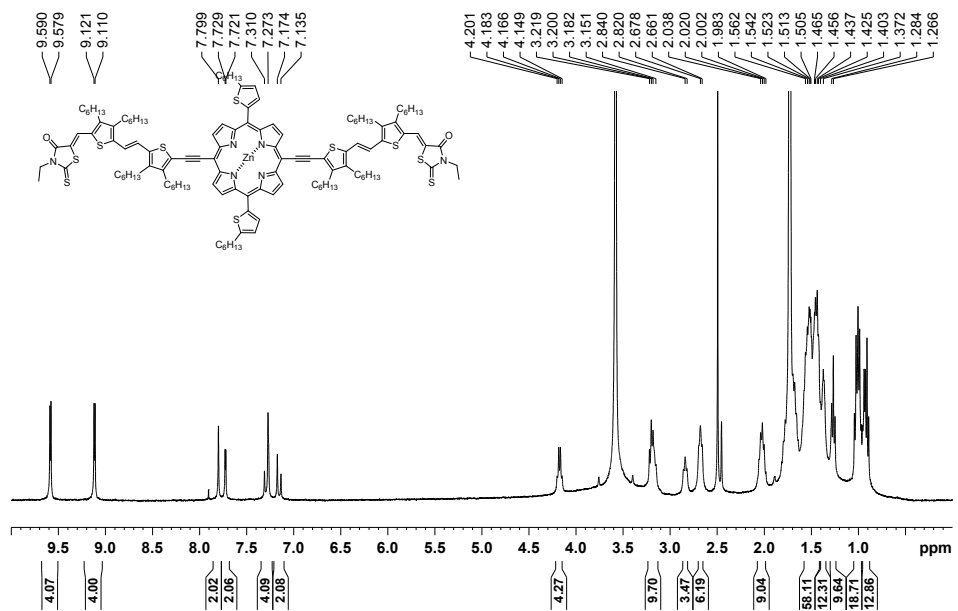


Figure S18. ^1H NMR spectrum (400 MHz, THF-D8) of **1b**.

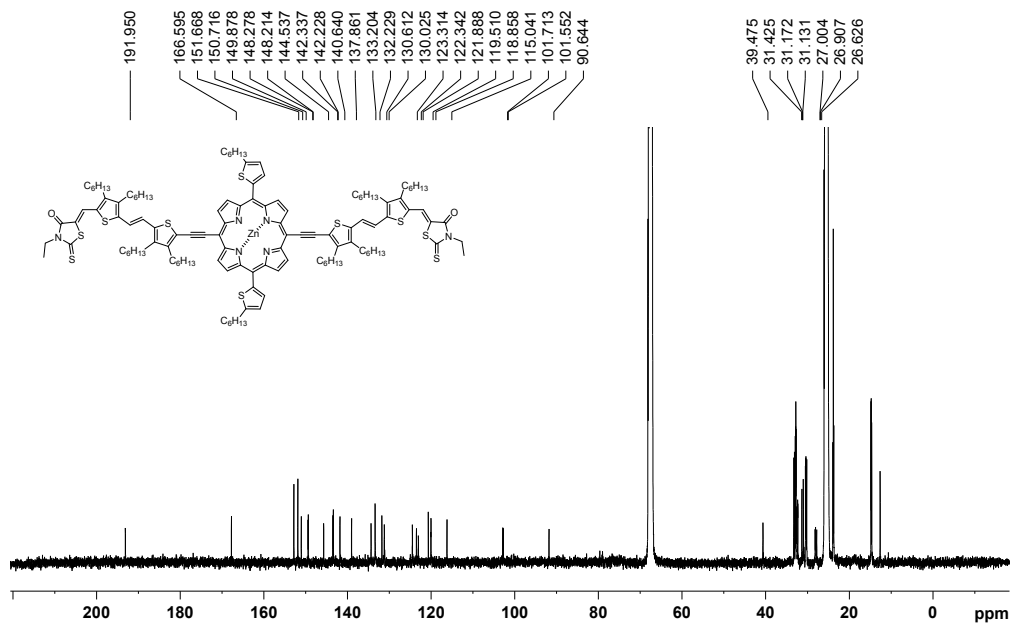


Figure S19. ^{13}C NMR spectrum (100 MHz, THF-D8) of **1b**.

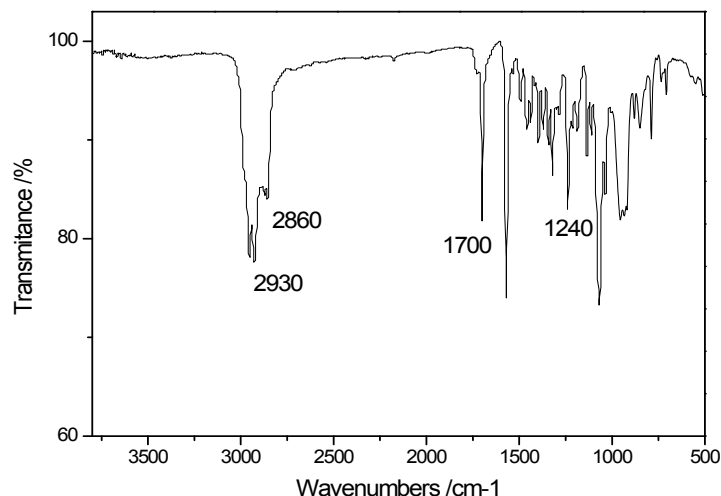


Figure S20. FT-IR spectrum of compound **1b**.

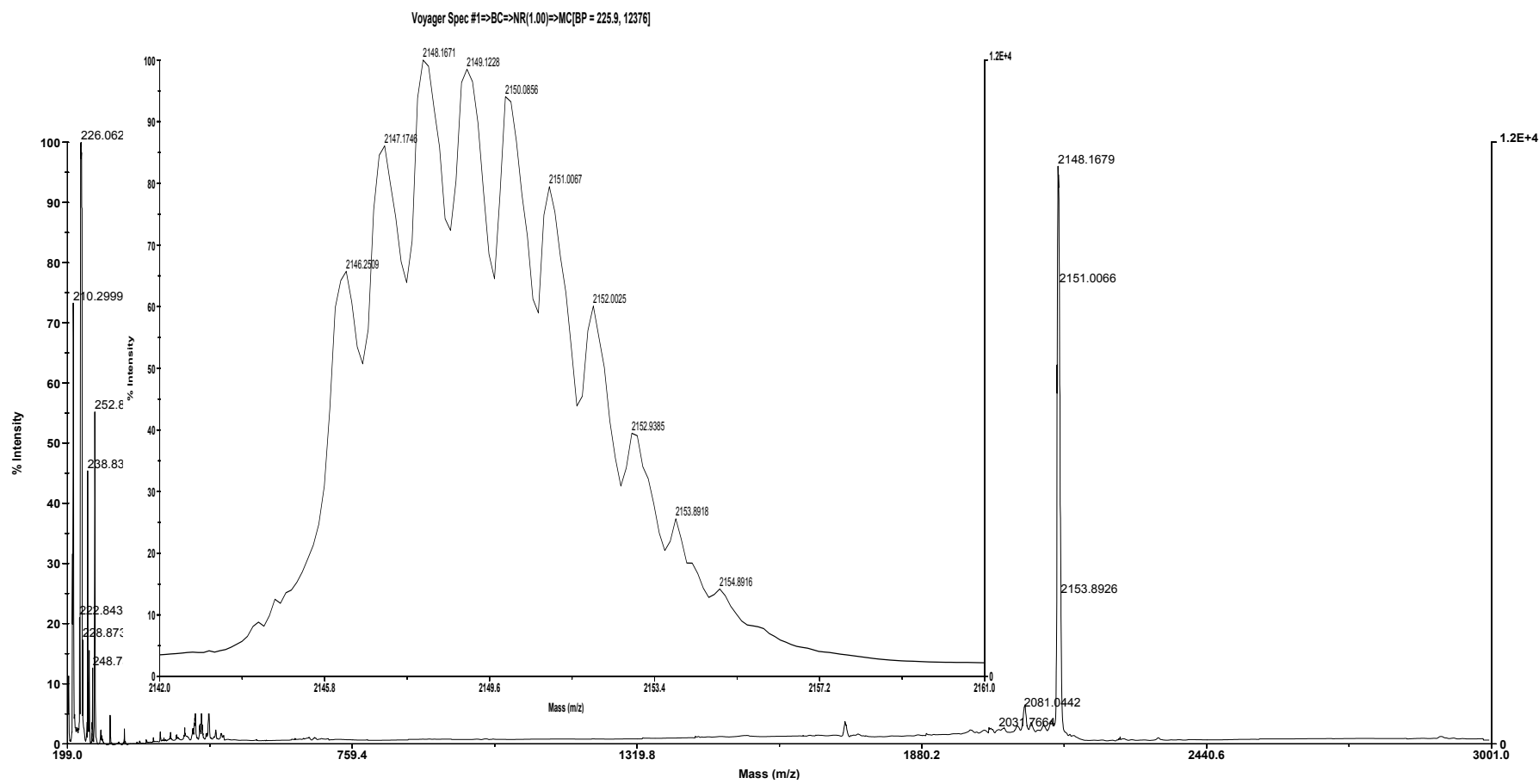


Figure S21. MALDI-TOF MS spectrum of compound **1b** (Matrix: Dithranol).

3. Thermogravimetric analysis

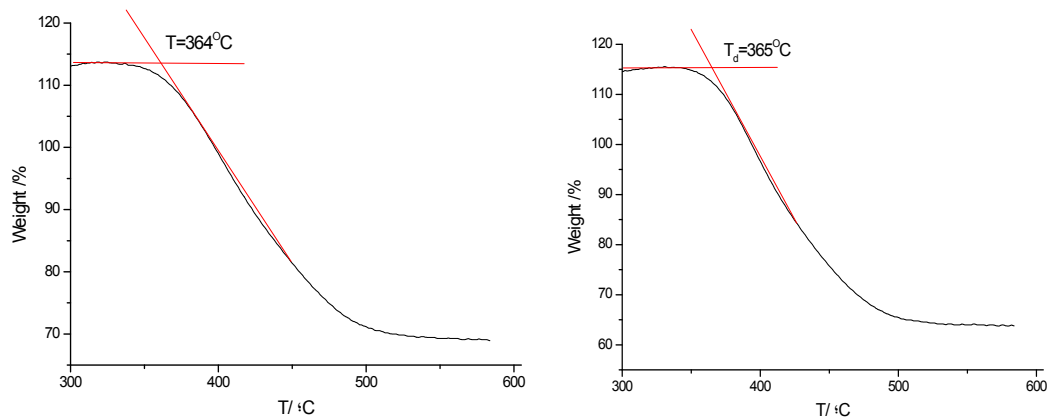


Figure S22. Thermogravimetric analysis of **1a** (left) and **1b** (right).

4. UV-Visible and emission spectroscopies

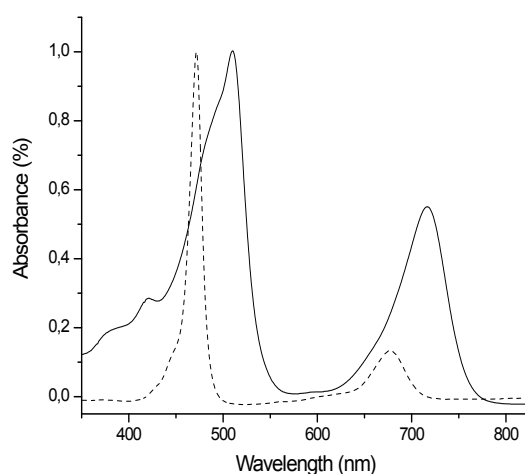


Figure S23. Normalized UV-Vis absorption spectra of compounds **1a** (—) and precursor **8a** (---) 10^{-5} M in THF.

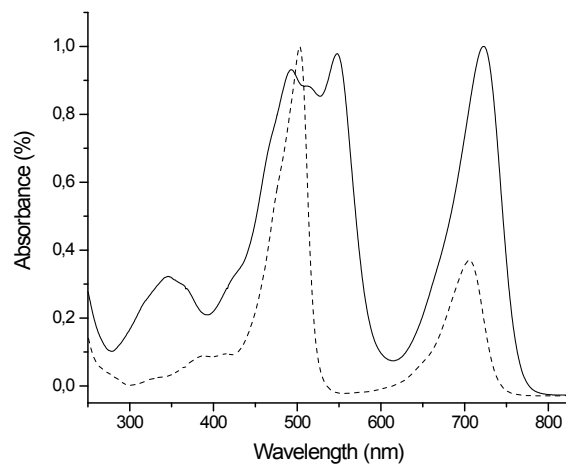


Figure S24. Normalized UV-Vis absorption spectra of compound **1b** (—) and precursor **8b** (---) in 10^{-5} M THF.

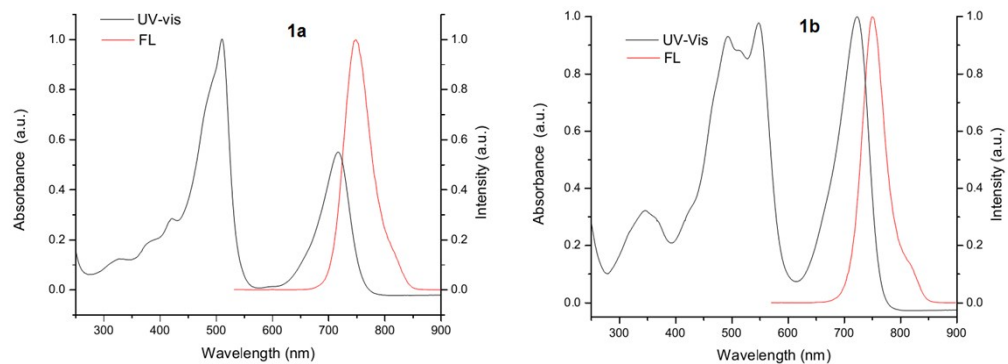


Figure S25. Normalized absorption and fluorescence spectra of **1a** and **1b** to estimated E_{o-o}

5. Cyclic Voltammetry and Square Wave plots.

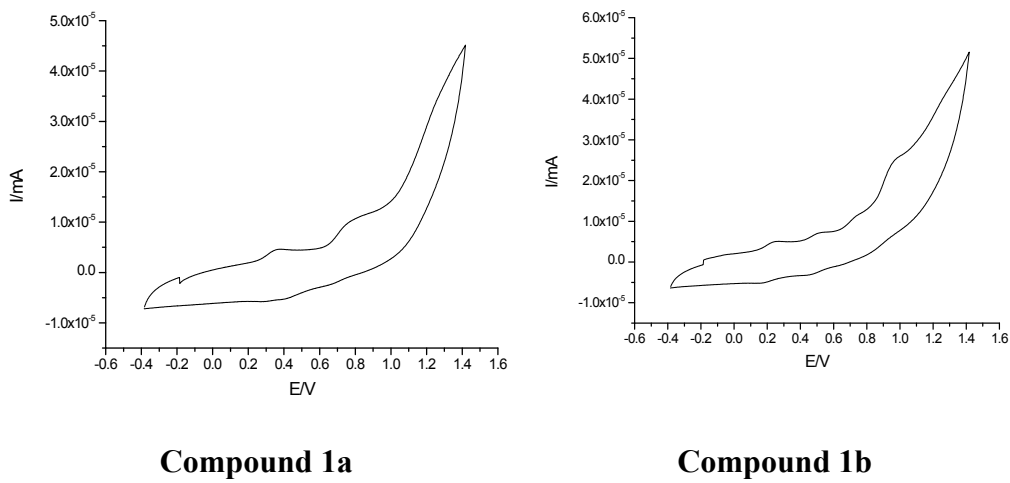


Figure S26. Cyclic Voltammetry of compound **1a** and **1b** (referred to Fc/Fc^+).

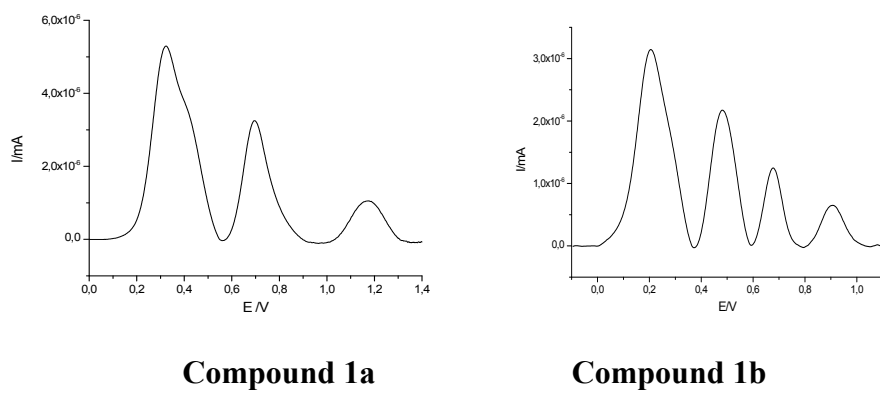


Figure S27. OSWV of **1a** and **1b** (anodic window) (referred to Fc/Fc^+).